文章编号：1001－9014(2019)04－0403－05

DOI:10.11972/j.issn.1001－9014.2019.04.002

Circular single-photon avalanche diode with high premature edge breakdown and extended spectrum

JIN Xiang-Liang[1,2*], ZENG Duo-Duo[1], PENG Ya-Nan[1], YANG Hong-Jiao[1], PU Hua-Yan[3], PENG Yan[3*], LUO Jun[3]

(1. School of Physics and Optoelectronics, Xiangtan University, Xiangtan 411105, China;
2. School of Physics and Electronics, Hunan Normal University, Changsha 410081, China;
3. School of Mechatronic Engineering and Automation, Shanghai University, Shanghai 200444, China)

Abstract: This paper presents a 0.18 μm complementary metal-oxide-semiconductor (CMOS) technology high premature edge breakdown, extended spectrum and low dark count rate circular single-photon avalanche diode (SPAD) which together form a novel wide spectrum fluorescence correlation spectroscopy (FCS) detector. The circular device consists of a p+/deep n-well junction, a p-well guard-ring, and a poly guard-ring. Simulations on a Silvaco TCAD 3D device also show that the 10 μm-diameter circular p+/deep n-well SPAD device has high premature edge breakdown characteristics. Moreover, compared to the SPAD p+/n-well junction, the p+/deep n-well junction has a longer wavelength response and spectral expansion. The device achieves wide spectral sensitivity enabling greater than 40% photon detection probability from 490 to 775 nm wavelength at 0.5 V excess bias. The circular p+/deep n-well SPAD has fine avalanche breakdown (15.14 V) and a low dark count rate of 638 Hz at 25℃.

Key words: single-photon avalanche diode(SPAD), premature edge breakdown (PEB), dark count rate(DCR), spectral expansion

PACS: 85.60.Bt, 85.60.Dw, 85.30.-z.

高边缘击穿和扩展光谱的圆形单光子雪崩二极管

金湘亮[1,2*]，曾朵朵[1]，彭亚男[1]，杨红姣[1]，蒲华燕[3]，彭 艳[3*]，罗 均[3]

(1. 湘潭大学 物理与光电工程学院,湖南 湘潭 411105;
2. 湖南师范大学 物理与电子科学学院,湖南 长沙 410081;
3. 上海大学 机电工程与自动化学院,上海 200444)

摘要:介绍了一种0.18 μm互补金属氧化物半导体(CMOS)技术的新型宽光谱荧光相关谱探测器,其为高边缘击穿、扩展光谱和低暗计数率的圆形单光子雪崩二极管(SPAD).该器件由p+/deep n-well结,p-well保护环和多晶硅保护环组成.通过Silvaco TCAD 3D器件仿真,直径为10 μm的圆形p+/deep n-well SPAD器件具有较高边缘击穿特性.此外,p+/deep n-well结SPAD比p+/n-well结SPAD具有更长的波长响应和扩展光谱响应范围.该器件在0.5 V过量偏压下,可在490～775 nm波长范围内实现超过40%的光子探测率.该圆形p+/deep n-well SPAD器件在25℃时具有较好雪崩击穿为15.14 V,具有较低暗计数率为638 Hz.

关 键 词:单光子雪崩二极管(SPAD);边缘击穿;暗计数率;光谱扩展

中图分类号:TN313　　**文献标识码**:A

Received date: 2018-12-06, **revised date**: 2019-05-24　　**收稿日期**:2018-12-06, **修回日期**:2019-05-24

Foundation items: Supported by National Natural Science Foundation of China (61774129, 61827812, 61704145), and Changsha Science and Technology Project(kq1801035)

Biography: JIN Xiang-Liang (1974-), male, Professor. Research interests include MEMS and readout circuit design, CMOS image sensor design, ESD, and mixed-mode application-specific integrated circuits.

* **Corresponding author**: E-mail: jinxl@hunnu.edu.cn, pengyan@shu.edu.cn

Introduction

Single-photon avalanche detectors (SPADs) are PN junction devices biased by Geiger Mode, i. e., devices with bias voltage beyond their breakdown voltage. The electric field in the SPAD multiplication region is so intense that a single photon carrier is sufficient to begin a self-maintained avalanche by impact ionization due to the generation of photons, which creates high pulse signaling. A single photon can thus be detected by the associated electronic circuitry[1]. SPADs can detect the arrival resolution of individual photons in dozens of picoseconds time[2]. Photon-counting devices are widely used in quantum key distribution systems for the purposes of single molecule detection[3-4]. Researchers have developed solid-state SPADs as CMOS technologies suited to an array of science and engineering applications[5]. CMOS SPADs[6] have been successfully applied in low-noise, high timing resolution, and high dynamic ranges[7].

Recent scholars have focused on developing new SPADs with low DCR[8-9], wide spectral response[10-11], small pixel size[12], and low breakdown voltage[13]. New CMOS SPAD designs tend to center on enhanced fill factor, reduced edge breakdown, and increased long-wavelength detection. The SPAD with a p +/deep n-well junction of deep sub-micrometer CMOS technology produces high dark noise by tunneling while minimizing photon detection efficiency (PDE). However, the low doping concentration of the deep n-well makes the p +/deep n-well junction deeper and the detected wavelength move towards a longer wavelength.

A variety of SPAD shapes (e. g., circular, octagonal, ellipsoidal) have been proposed to improve the device performance[14]. In this work, we fabricated the proposed SPAD in a 0.18 μm CMOS process with a 10 μm active diameter. The SPAD's circular structure effectively reduces the electric field concentration at corners, and thus effectively prevents edge breakdown and increases the fill factor.

1 P +/deep n-well versus p +/n-well junction SPAD

The circular device consists of a p +/n-well junction, a p-well guard-ring, and a poly guard-ring. A cross-section of the SPAD structure is shown in Fig. 1. The SPAD has a narrow depletion layer and a strong electric field, which raises the avalanche breakdown probability. The spectral response of the device is biased towards the blue band. The p-well, as a guard ring, merges with the depletion layer when the p +/n-well SPAD is relatively small in size. As the breakdown voltage of the device increases, the p +/n-well loses its efficacy as the diameter of the source area is 5 μm[15]. In this study, we used a source area of 10 μm.

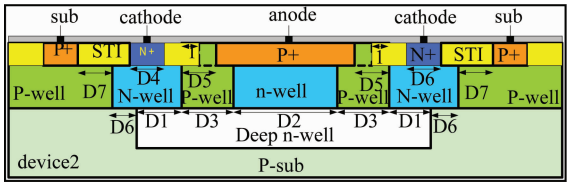

Fig. 1 P +/n-well junction SPAD structure
图 1 P +/n 阱结 SPAD 器件结构

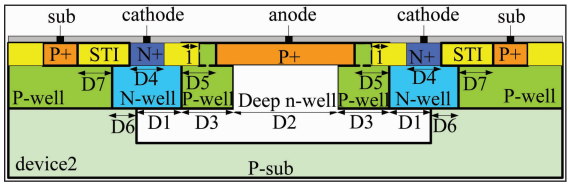

Fig. 2 P +/deep n-well junction SPAD structure
图 2 P +/深 n 阱结 SPAD 器件结构

The p +/deep n-well junction SPAD has a wide wavelength response to suit the wide-spectrum detector, because electrons generated in the wide junction trigger the avalanche with high impact ionization possibilities. A cross-section of the SPAD structure is shown in Fig. 2. The deep n-well with a small doping concentration in the structure replaces the n-well, and the p +/deep n-well forms an active multiplication junction. The device has a wide depletion layer which allows for extended spectrum response. The p +/deep n-well and p +/n-well junction of SPAD structure we tested are described in Table 1.

The two devices retain the STI around the protection ring to reduce the width of the protection ring. The Silvaco TCAD simulation of electric field are shown in Fig. 3, indicating that the protection ring prevents edge breakdown. Compared with P +/Deep n-well junction SPAD, the doping concentration of P +/N-well junction SPAD has been increased, the depletion layer has been narrowed, and the breakdown voltage has been decreased.

As shown in Fig. 4, the photoreceptor depth of the p +/n-well junction SPAD and p +/deep n-well junction SPAD is 0.2-0.6 μm and 0.2-0.9 μm, respectively. Deeper junctions absorb photons at longer wavelengths providing improved PDE toward the red band of the spectrum. The 2D Silvaco TCAD simulation results show that the p +/deep n-well junction SPAD has the wider spectral response between them.

2 Octagonal versus circular SPAD

Two shapes of SPAD were tested in this study as per

Table 1 The size of p +/deep n-well and p +/n-well junction SPAD structure
表 1 P +/深 n 阱和 p +/n 阱 SPAD 结构尺寸表

Device name	D1 (μm)	D2 (μm)	D3 (μm)	D4 (μm)	D5 (μm)	D6 (μm)	D7 (μm)	Shape	PN junction
Circular p +/n-well SPAD	2.1	10	3	2.2	2.5	1.6	2.9	Circular	p +/n-well
Circular p +/deep n-well SPAD	2.1	10	3	2.2	2.5	1.6	2.9	Circular	p +/deep n-well

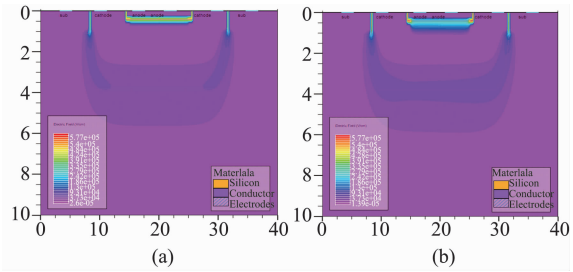

Fig. 3　Electric field in p +/n-well junction SPAD(a) and p +/deep n-well junction SPAD(b)
图 3　P +/n 阱结 SPAD(a)和 p +/深 n 阱结 SPAD(b)电场分布图

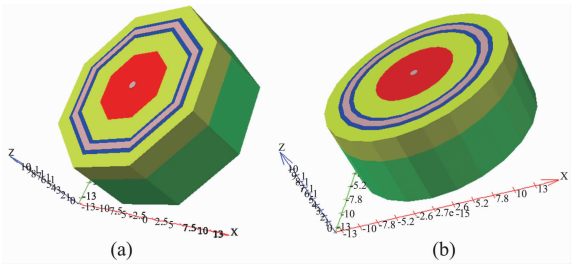

Fig. 5　Silvaco TCAD 3D device simulation for octagonal (a) and circular (b) p +/deep n-well junction SPADs
图 5　八边形(a)和圆形 p +/深 n 阱结 SPAD(b)的 Silvaco TCAD 3D 器件仿真结构图

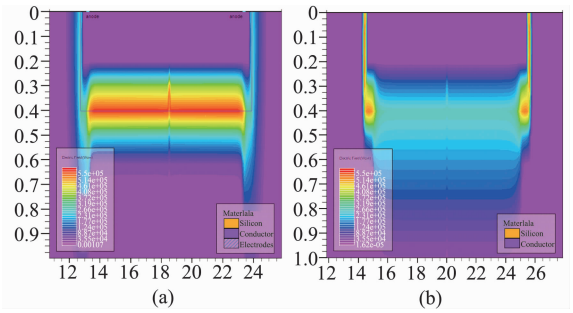

Fig. 4　PN junction electric field in p +/n-well junction SPAD(a) and p +/deep n-well junction SPAD(b)
图 4　P +/n 阱结 SPAD(a)和 P +/深 n 阱结 SPAD(b)的 PN 结电场分布图

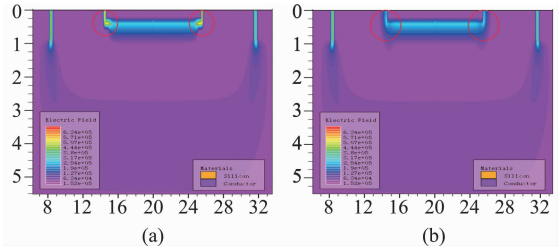

Fig. 6　Electric field in octagonal (a) and circular (b) p +/deep n-well junction SPADs
图 6　八边形 P +/深 n 阱(a)和圆形 P +/深 n 阱 SPAD(b)的剖面电场分布图

their effects on the edge breakdown. As shown in Fig. 5, we used a Silvaco TCAD 3D device to simulate the octagonal and circular p +/deep n-well junction SPADs. The electric field of the octagonal SPAD edge is greater than that of the circular SPAD edge, which is mainly due to the large curvature of the p-n junction and sharp SPAD shape. The octagonal and circular SPAD structure we tested are described in Table 2.

We found that the electric field of the octagonal SPAD edge is greater than that of the circular SPAD edge (red circle, Fig. 6). The circular shape SPAD reduces the electric field concentration and prevents premature edge breakdown.

3　Experiments and discussion

To optimize the structural shape and junction doping concentration of the SPAD device, we fabricated different SPADs in 0.18 μm CIS technology. A photomicrograph of the chip is shown in Fig. 7. The circular p +/n-well junction SPAD, circular p +/deep n-well junction SPAD, and octagonal p +/deep n-well junction SPAD are shown from left to right in Fig. 7.

A passive quench circuit was used to measure the dark count rate (DCR) of the SPADs; the measurement circuit is shown in Fig. 8. The cathode of the SPAD was connected to the voltage source $V_{Excess} + V_{Breakdown}$ and the anode to the ground at a 51 kΩ quenching resistance. The SPAD test platform and quenching circuits (Fig. 9) were measured for DCR in darkness.

Figure 9 shows a test platform which consists of three templates representing a DC power supply, digital oscilloscope, and the proposed SPAD plus quenching circuits, respectively.

The inverse I-V characteristics of the three SPADs were measured as shown in Fig. 10. The breakdown voltage of the circular p +/deep n-well junction SPAD, the octagonal p +/deep n-well junction SPAD, and the circular p +/n-well junction SPAD are approximately 15.14 V, 15.12 V, and 10.62 V, respectively (Fig. 10). The breakdown voltage of the circular p +/deep n-well junction SPAD is approximately 15.14 V, which exceeds the 13.9 V reported in the literature circular device[11] due to the 0.13 μm CMOS technology, in which the doping concentration is relatively large and the breakdown voltage is small. Under the same bias voltage and non-break-

Table 2　The size of octagonal and circular SPAD structure
表 2　八边形 SPAD 和圆形 SPAD 结构尺寸表

Device name	D1 (μm)	D2 (μm)	D3 (μm)	D4 (μm)	D5 (μm)	D6 (μm)	D7 (μm)	Shape	PN junction
Circular p +/deep n-well SPAD	2.1	10	3	2.2	2.5	1.6	2.9	Circular	p +/deep n-well
Octagonal p +/deep n-well SPAD	2.1	10	3	2.2	2.5	1.6	2.9	Octagonal	p +/deep n-well

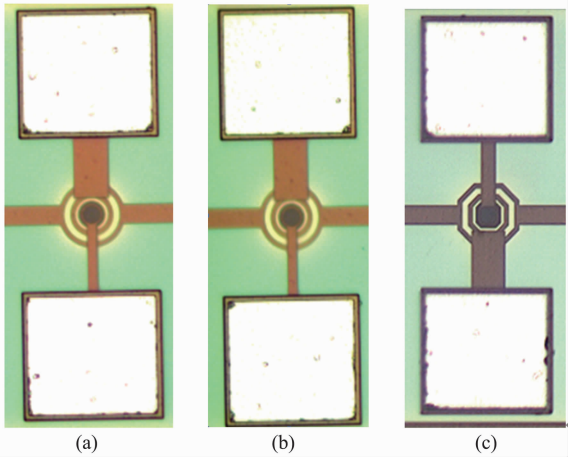

Fig. 7 Micrograph of SPADs fabricated in 0.18 μm CIS technology of (a) the circular p+/n-well junction, (b) the circular p+/deep n-well junction, and (c) the octagonal p+/deep n-well junction

图7 (a)圆形p+/n阱结SPAD,(b)圆形p+/深n阱结SPAD,(c)八边形p+/深n阱结SPAD的0.18 μm CIS技术芯片显微照片

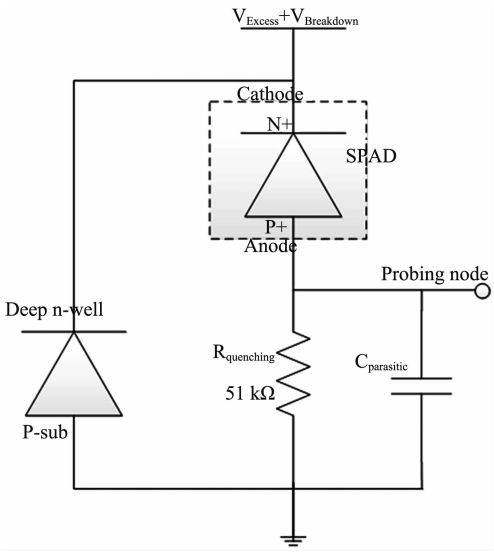

Fig. 8 Measurement circuit of the SPAD device

图8 SPAD器件测试电路图

down edge condition, the photocurrent of the circular p+/n-well junction SPAD is particularly large.

The DCR and bias voltage have linear relationship at room temperature (Fig. 11) due to the probability of avalanche breakdown and the generation of tunnel carriers. An excess bias voltage ranging from 0.1 V to 1 V was applied with a 0.1 V step. The DCR of the circular p+/n-well junction SPAD is much greater than that of the circular p+/deep n-well junction SPAD at the same excess bias voltage to the photosensitive junction concentration and high avalanche breakdown probability. At room temperature, the octagonal and circular p+/deep n-well junction SPAD DCRs are 112 Hz and 105 Hz, respec-

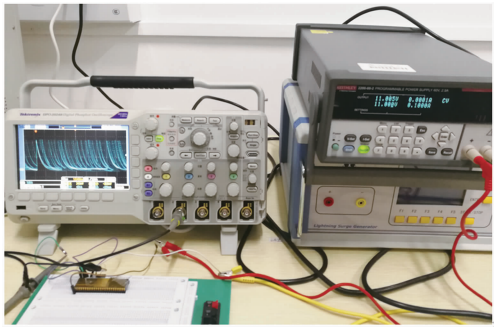

Fig. 9 Test platform of the SPAD with its quenching circuits

图9 SPAD被动淬灭电路测试平台

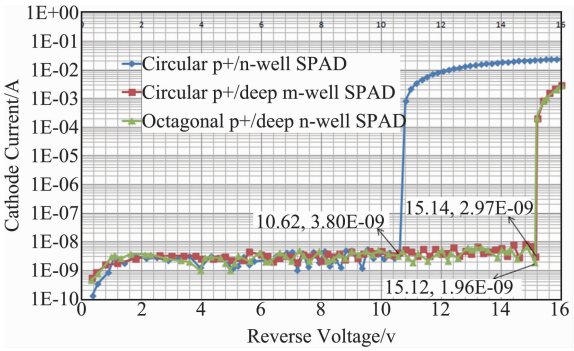

Fig. 10 SPAD breakdown voltage versus diameter for circular p+/n-well SPAD and circular p+/deep n-well SPAD and octagonal p+/deep n-well SPAD

图10 圆形p+/深n阱结SPAD,八边形p+/深n阱结SPAD和圆形p+/n阱结SPAD的电流电压特性曲线图

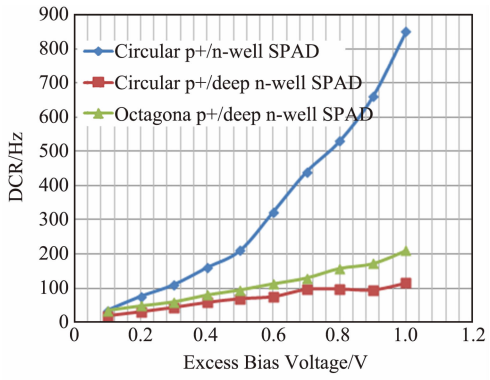

Fig. 11 SPAD DCR at varying excess bias voltage

图11 SPAD在过量偏压下的暗计数率测试图

tively, when the excess bias voltage is 1 V.

The photon detection probability (PDP), which is the ratio of the quantity of detected photons over the quantity of incident photons, was measured over a wavelength range from 400 nm to 1 100 nm at room temperature with an excess bias voltage of 500 mV. As shown in Fig. 12, the p+/n-well junction SPAD detected a wavelength range with maximum PDP of 565 nm, or 16%.

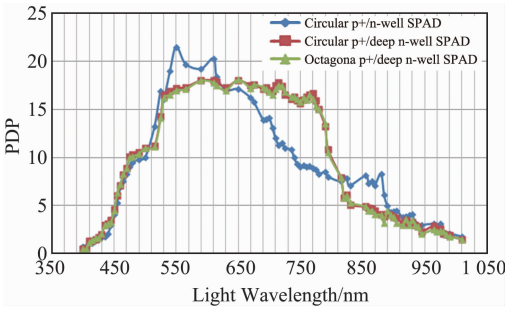

Fig. 12　Spectral responses of three different SPAD structures at $T = 25℃$

图 12　三种不同 SPAD 在常温下的光谱响应测试图

The circular p +/deep n-well junction SPAD has longer wavelength response with a peak value wavelength up to 775 nm. The device achieves spectral response sensitivity with above 40% PDP from 490 to 775 nm wavelength, and the spectral response is enlarged.

The proposed circular SPAD device with p +/deep n-well junction allows active multiplying junctions with deep n-well shallow n-type doping, increases the depletion layer width compared to the other SPADs, and detects light over a wide spectrum and long wavelength; however, its PDP is relatively low. As shown in the diagram, the loss region is relatively thick and it is to some extent beneficial to enhancing the spectral response.

4　Conclusion

A circular p +/deep n-well junction SPAD implemented in a 0.18 μm CMOS technology was introduced in this paper. The circular device consists of a p +/deep n-well junction, a p-well guard-ring, and a poly guard-ring. The circular p +/deep n-well junction SPAD, octagonal p +/deep n-well junction SPAD, and circular p +/n-well junction SPAD were compared to find that the p +/deep n-well junction SPAD has extended spectrum response characteristics relative to the p +/n-well junction SPAD; the former device achieves wide spectral sensitivity with above 40% PDP from 490 to 775 nm wavelength at 0.5 V excess bias. Theoretical analysis, simulation via Silvaco TCAD 3D device, and measurements together indicated that the avalanche breakdown voltage of the circular SPAD device with 10 μm diameter is 15.14 V. It also shows high premature edge breakdown and low DCR of 638 Hz at 25℃.

References

[1] YANG Hong-Jiao, JIN Xiang-Liang. Minimization design of guard ring size of p- well / DNW single photon avalanche diode [J]. *Journal of Infrared and Millimeter Waves*(杨红姣, 金湘亮. p-well/DNW 单光子雪崩二极管保护环的最小化设计. **红外与毫米波学报**,2018, **37**(5): 527 - 532.

[2] Pancheri L, Massari N, Stoppa D. SPAD image sensor with analog counting pixel for time-resolved fluorescence detection [J]. *Electron Devices, IEEE Transactions on* , 2013, **60**(10):3442 - 3449.

[3] Takeuchi S, Kim J, Yamamoto Y, *et al*. Development of a high-quatum efficiency single-photon counting system [J]. *Appl. Phys. Lett.* 1999, **74**(8):1063 - 1065.

[4] Cova S, Ghioni M, Lacaita A, *et al*. Avalanche photodiodes and quenching circuits for single-photon detection [J]. *Appl. Opt.* 1996, **35**(12):1956 - 1976.

[5] Karami M A, Gersbach M, Yoon H J, *et al*. A new single-photon avalanche diode in 90nm standard CMOS technology [J]. *Optics Express*, 2010, **18**(21):22158.

[6] Rochas A , Gani M , Furrer B , *et al*. Single photon detector fabricated in a complementary metal - oxide - semiconductor high-voltage technology[J]. *Review of Scientific Instruments*, 2003, **74**(7):3263.

[7] Niclass C, Rochas A, Besse P A *et al*. Design and Characterization of a CMOS 3-D Image Sensor Based on Single Photon Avalanche Diodes [J]. *J. Solid-State Circuits*, 2005, **40**(9):1847 - 1854.

[8] YANG Jia, JIN Xiang-Liang, YANG Hong-Jiao, et al. Design and analysis of a novel low dark count rate SPAD [J]. *Journal of Infrared and Millimeter Waves*(杨佳,金湘亮,杨红姣. 一种新型低暗计数率单光子雪崩二极管的设计与分析, **红外与毫米波学报**),2016,**35**(4): 394 - 397.

[9] Leitner T , Feiningstein A , Turchetta R , *et al*. Measurements and simulations of low dark count rate single photon avalanche diode device in a low voltage 180 nm CMOS image sensor technology [J]. *IEEE Transactions on Electron Devices*, 2013,**60**(6):1982 - 1988.

[10] Mandai S, Fishburn M W, Maruyama Y, *et al*. A wide spectral range single-photon avalanche diode fabricated in an advanced 180 nm CMOS technology[J]. *Optics Express*, 2012,**20**(6):5849 - 57.

[11] Veerappan C , Charbon E . A substrate isolated CMOS SPAD enabling wide spectral response and low electrical crosstalk [J]. *IEEE Journal of Selected Topics in Quantum Electronics*, 2014,**20**(6):1 - 7.

[12] Gyongy I , Davies A , Gallinet B , *et al*. Cylindrical microlensing for enhanced collection efficiency of small pixel SPAD arrays in single-molecule localisation microscopy [J]. *Optics Express*, 2018, **26**(3): 2280 - 2291.

[13] Tseng C K, Chen K H, Chen W T, *et al*. A high-speed and low-breakdown-voltage silicon avalanche photodetector[J]. *IEEE Photonics Technology Letters*, 2014,**26**(6):591 - 594.

[14] Moreno-Garcia M, del Rio R, Guerra O, *et al*. 5 × 5 SPAD matrices for the study of the trade-offs between fill factor, dark count rate and crosstalk in the design of CMOS image sensors [C]. *Microelectronics and Electronics (PRIME)*,2014, 1 - 4.

[15] Faramarzpour N, Deen M J, Shirani S, *et al*. Fully integrated single photon avalanche diode detector in standard CMOS 0.18 μm technology[J]. *IEEE Transactions Electron Devices*, 2008, **55**(3):760 - 767.

[16] Richardson J A , Webster E A G , Grant L A , *et al*. Scaleable single-photon avalanche diode structures in nanometer CMOS technology [J]. *IEEE Transactions on Electron Devices*, 2011, **58**(7):2028 - 2035.